

Supporting Information for Vibrational Energy Redistribution in Crystalline Nitromethane simulated by Ab initio Molecular Dynamics

Meilin Lu^{1, 2}, Zhaoyang Zheng^{2}, Gangbei Zhu², Yuxiao Wang¹, Yanqiang Yang^{1, 2*}*

¹ School of Physics, Harbin Institute of Technology, Harbin 150001, China

² National Key Laboratory of Shock Wave and Detonation Physics, Institute of Fluid Physics, China Academy of Engineering Physics, Mianyang 621900, China.

* Correspondence should be addressed to Yanqiang Yang (email: yqyang@hit.edu.cn) and Zhaoyang Zheng (email: zhengzy@yinhe596.cn).

Computational details

Figure S1. Comparison of SED spectra of CH stretching modes (M1-M3) in this work with our previous one.

Figure S2. Relaxation of all the excited vibrational modes.

Figure S3. Evolution of the unexcited vibrational modes' energy within the first 1 ps after the selective excitations of M1-M8.

Figure S4. Evolution of the unexcited vibrational modes' energy within the first 1 ps after the selective excitations of M9-M14.

Figure S5. The SED spectra of the direct daughter modes in the first picosecond after the 14 selective excitations.

Computational details

The electronic wave functions were expanded by plane wave basis with a kinetic energy cutoff of 800 eV and all atoms were relaxed until atomic forces were less than 0.01 eV/Å. The Brillouin zone is sampled by $6 \times 5 \times 3$ grids for structural optimization and only Γ -point was used in phonon calculation and molecular dynamic simulation. Five configurations were taken independently from the thermal equilibrium by Canonical ensemble (NVT) MD performed for more than 10 picoseconds. Time step in the MD was 0.4 fs and the microcanonical ensemble (NVE) MD simulations was performed to the system for 30000 steps (12 ps) to simulate the vibrational energy redistribution processes.

In the selective excitation, normal momentum of all the four-fold degenerate lattice modes corresponding to one molecular vibration i were set to be $r_i \hbar \omega_i$. Amount of the injected energy affects the transfer rates and after the pre-tests, the coefficient r_i were assigned to be 0.15 for M1-M3 and 0.75 for M4-M14. The excitation condition such as the injected energy and temperature would influence the specific VER rates and efficiencies, but won't change the underlying mechanisms of vibrational coupling which are intrinsic and inherent, as shown in Figure S1. When calculating the evolution of some mode's energy percentage, several values are slightly less than zero after the background subtraction owing to the limitation of the sampling number. They are briefly approximated to zero.

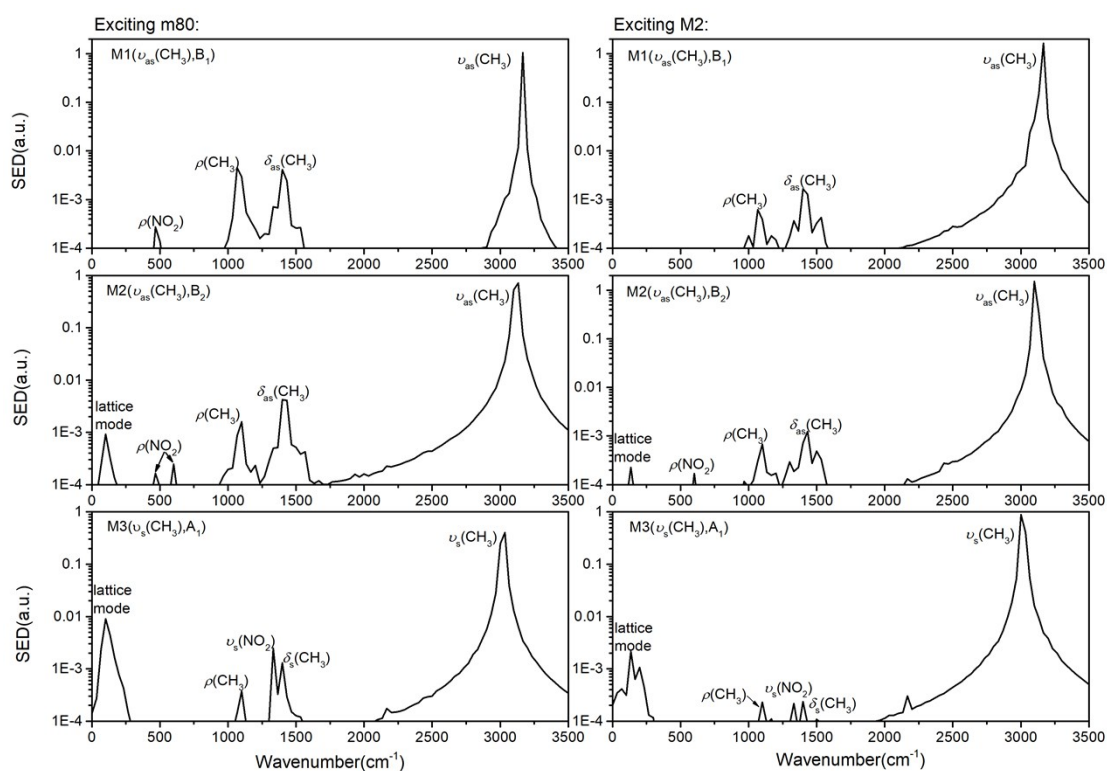


Figure S1. Comparison of SED spectra of CH stretching modes (M1-3) in this work (right) with our previous one (left)

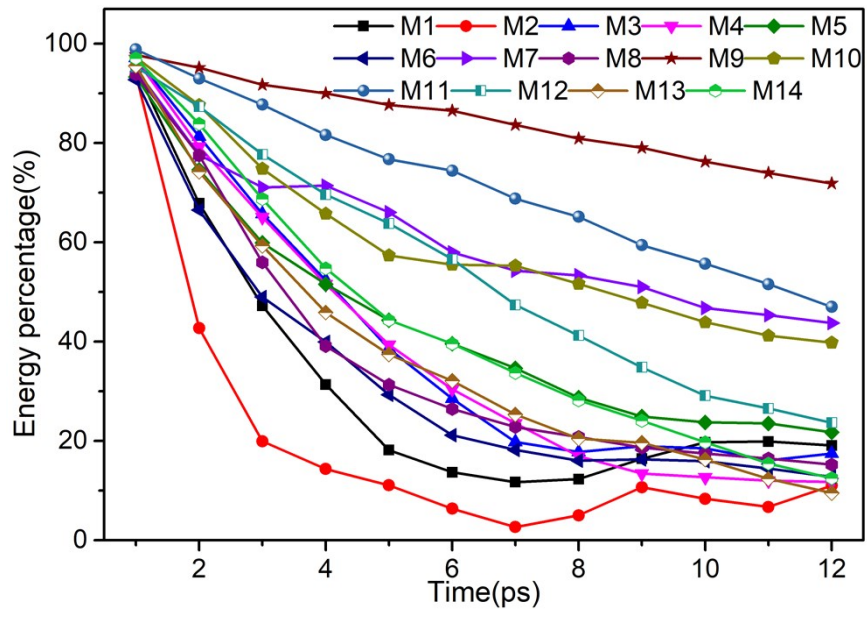


Figure S2. Relaxation of all the excited parent modes

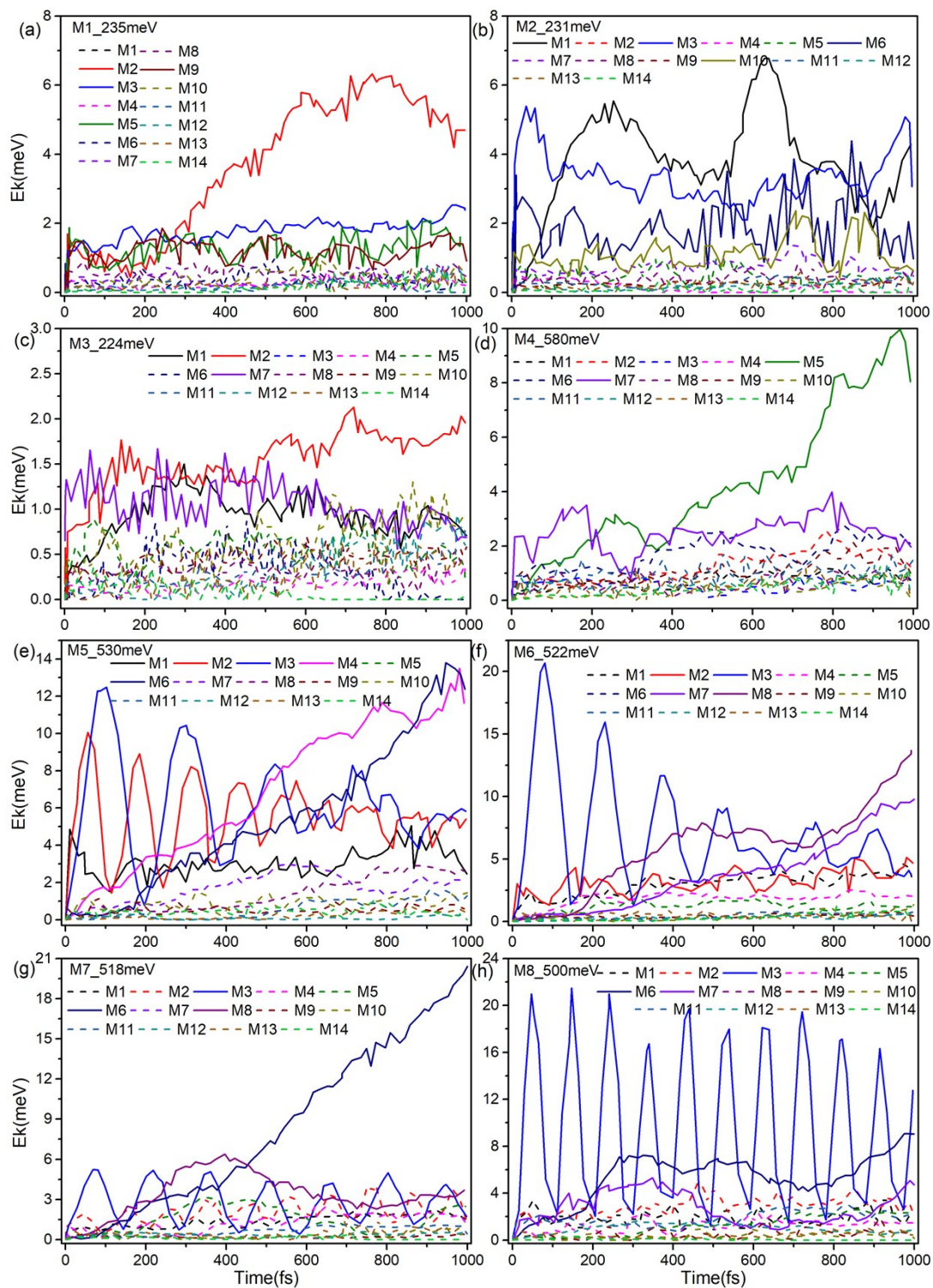


Figure S3. Evolution of the other vibrational modes' energy within the first 1 ps after the selective excitations of M1-M8.

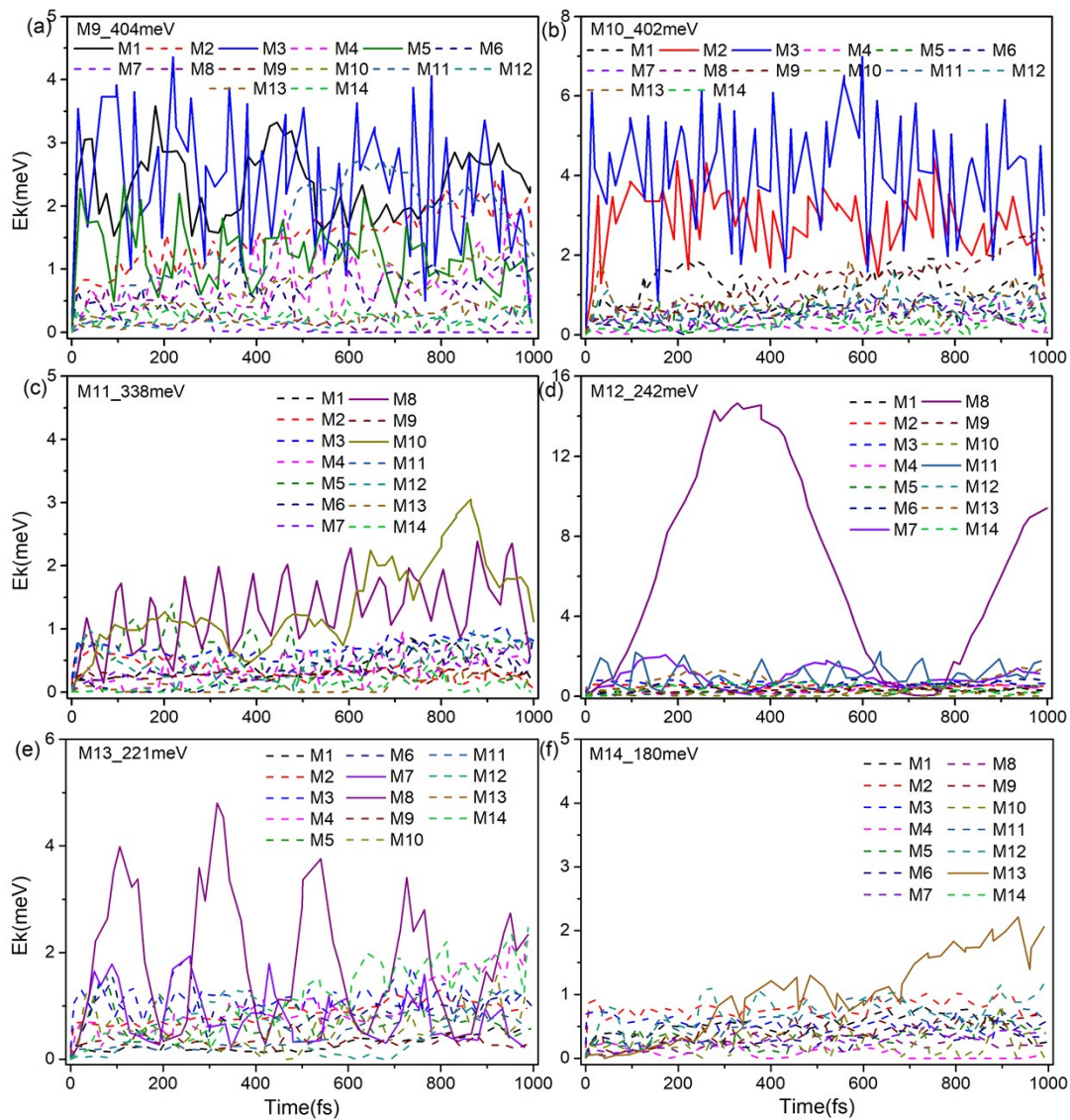
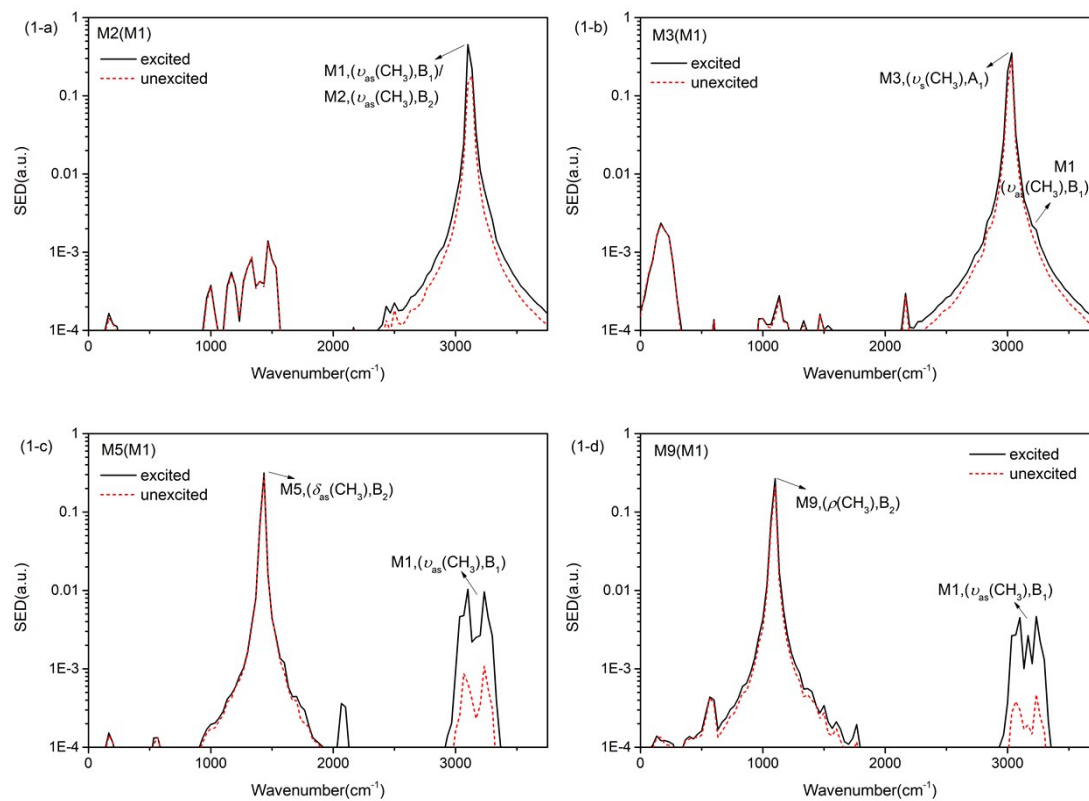
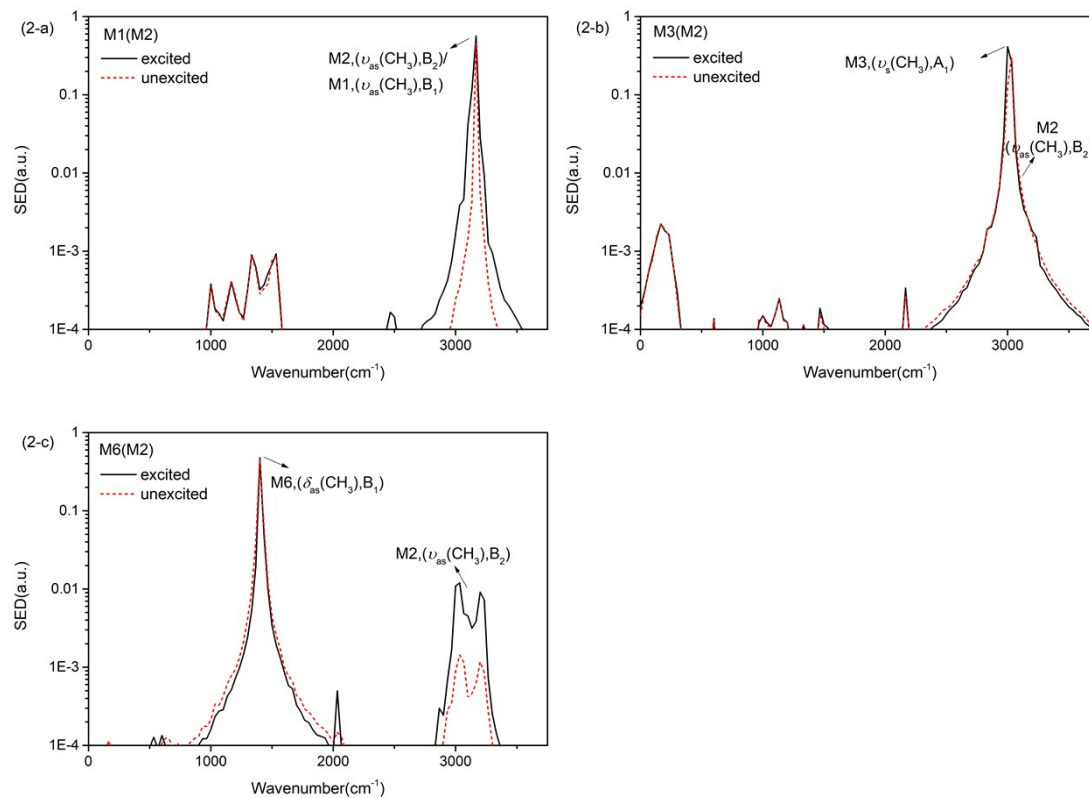


Figure S4. Evolution of the other vibrational modes' energy within the first 1 ps after the selective excitations of M9-M14.

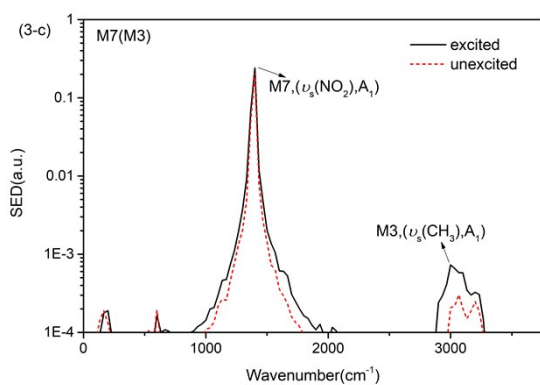
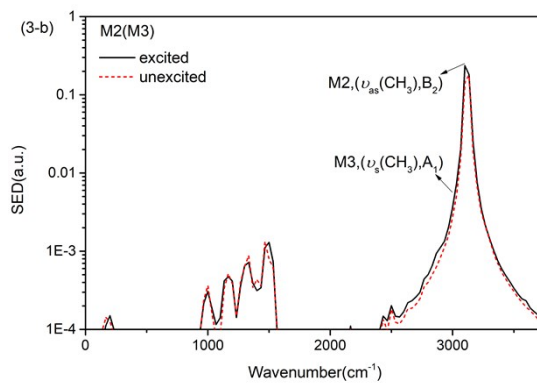
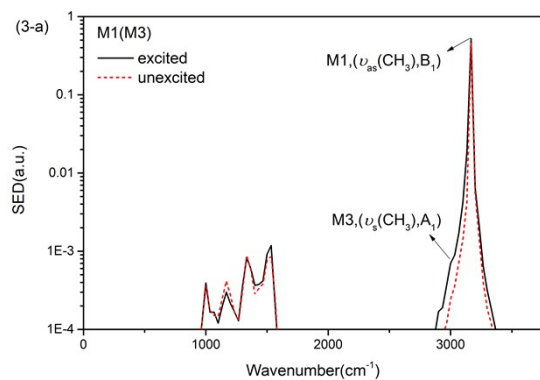
PM M1:



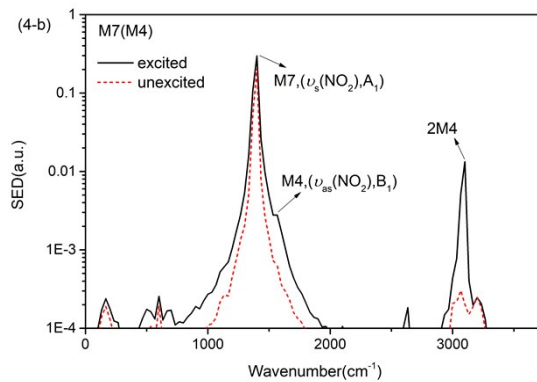
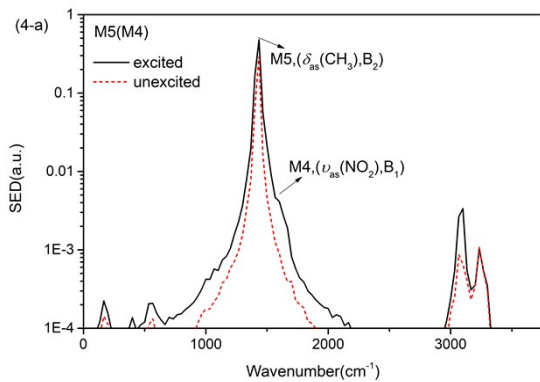
PM M2:



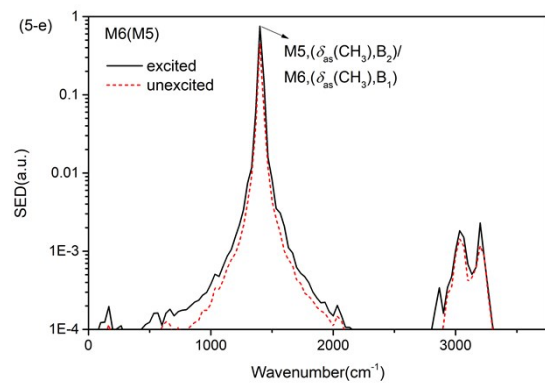
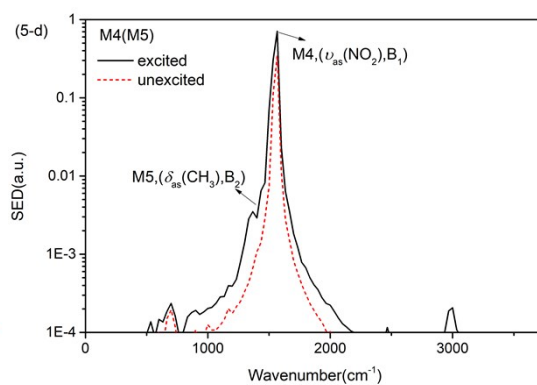
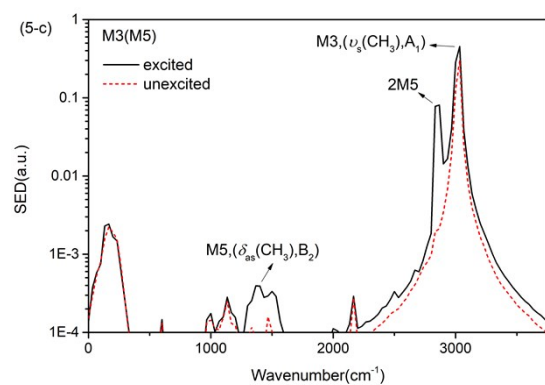
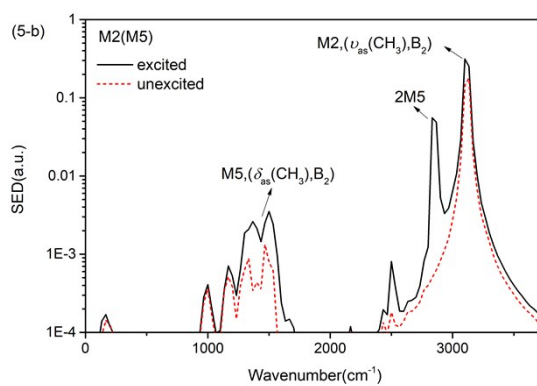
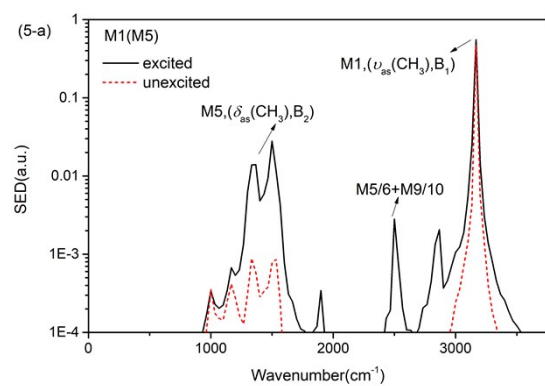
PM M3:



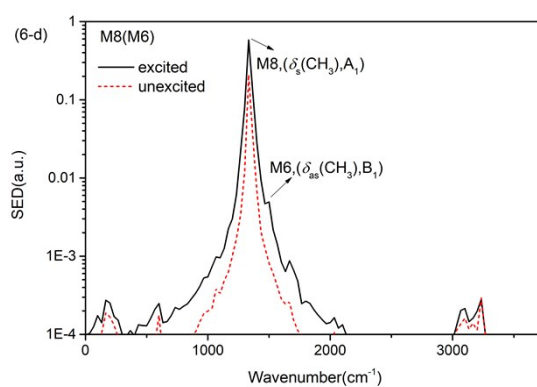
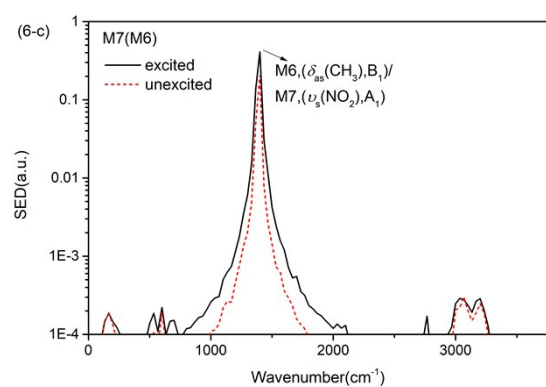
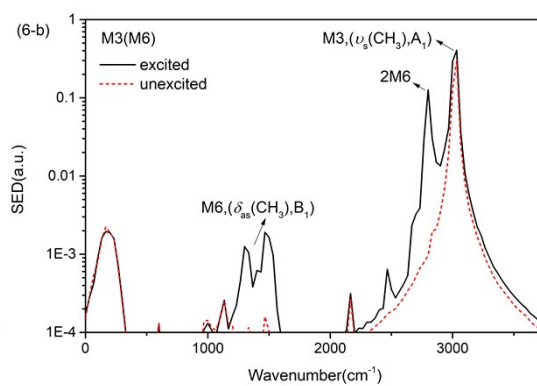
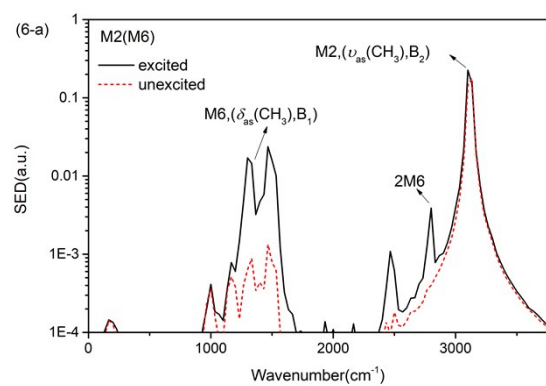
PM M4:



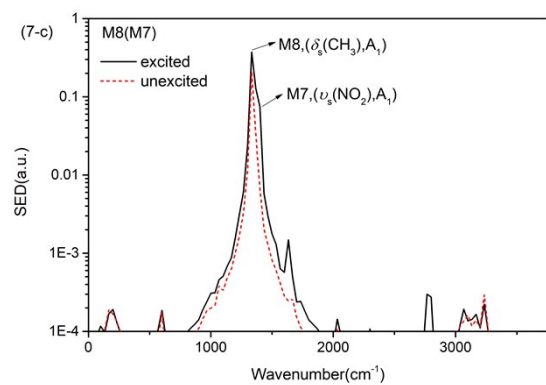
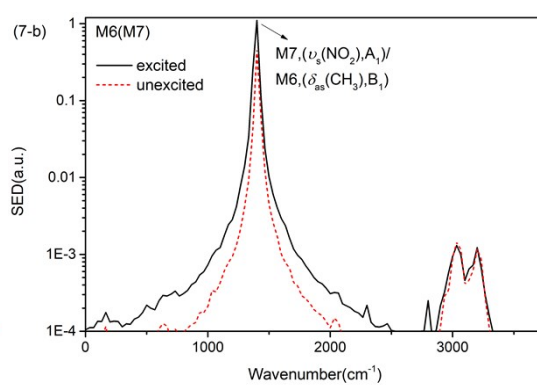
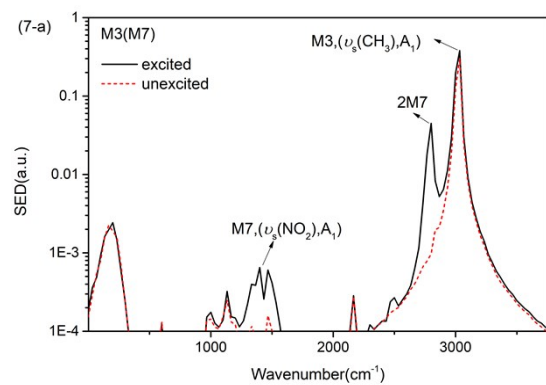
PM M5:



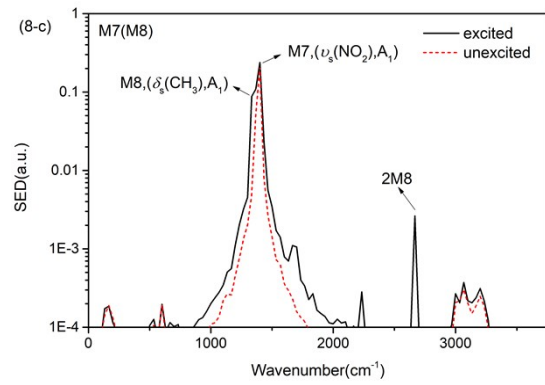
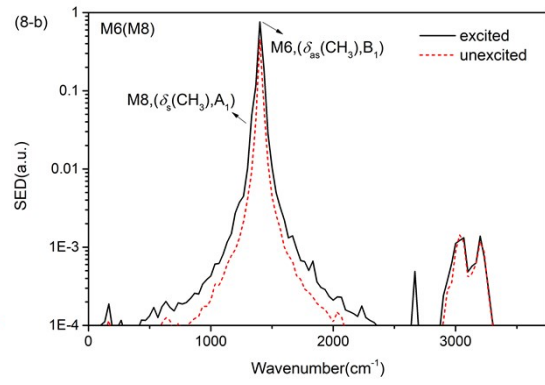
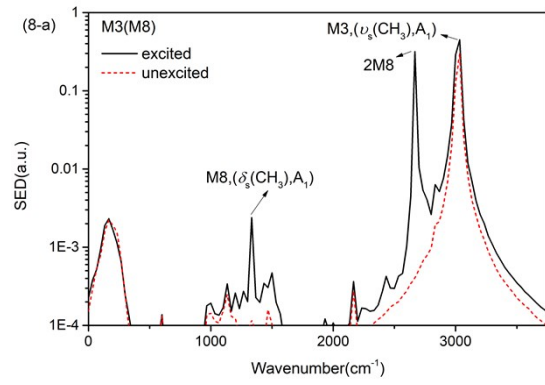
PM M6:



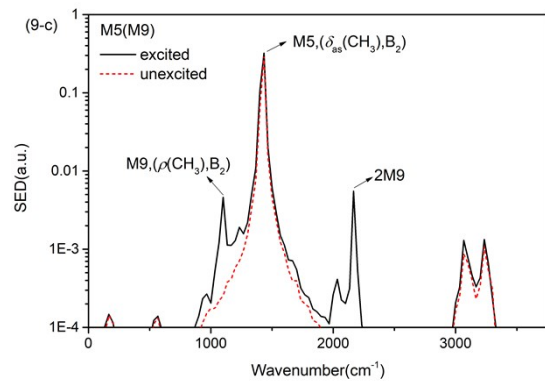
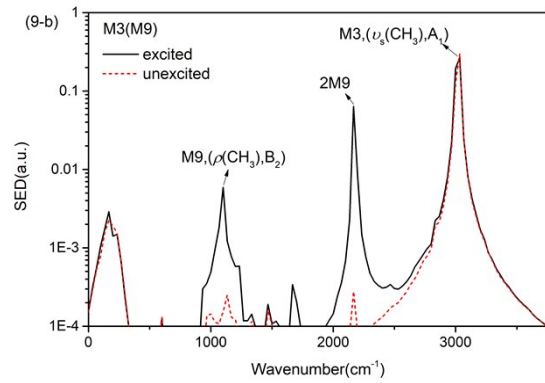
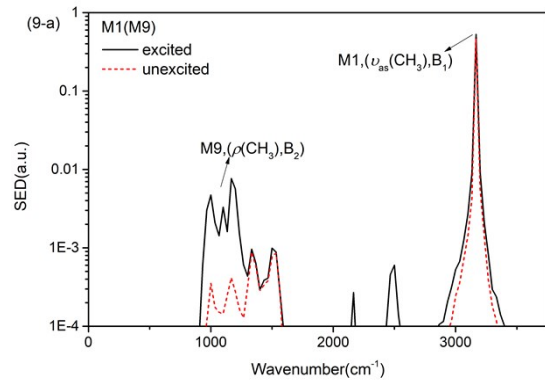
PM M7:



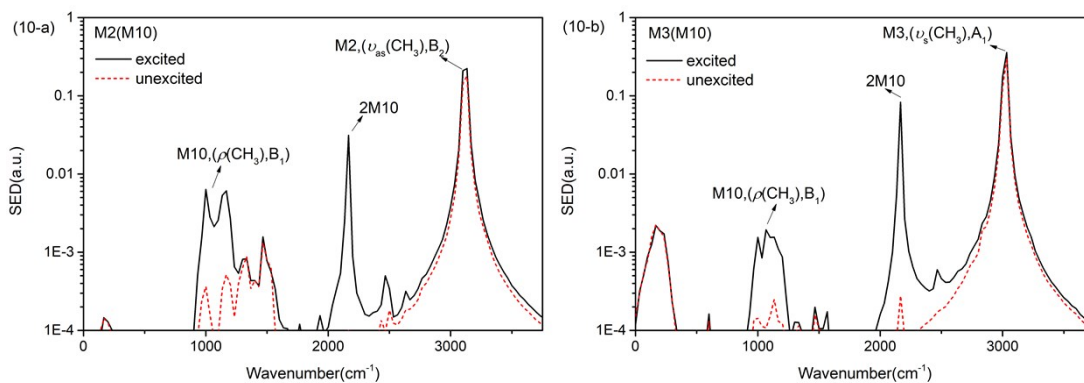
PM M8:



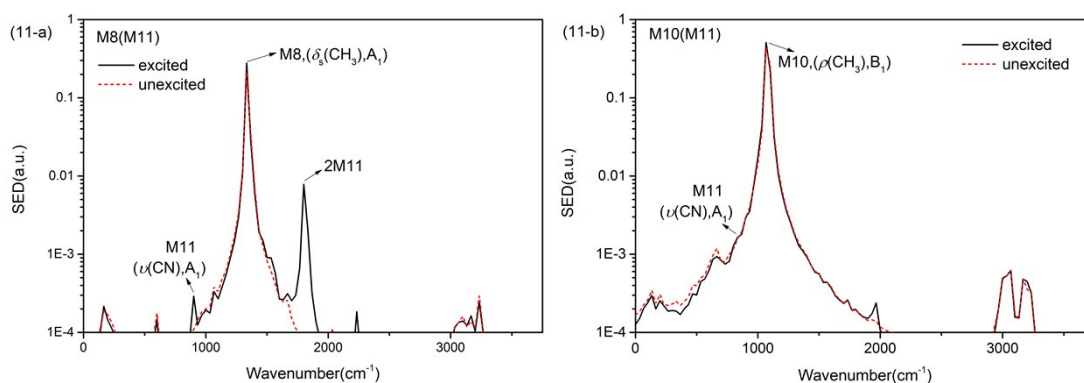
PM M9:



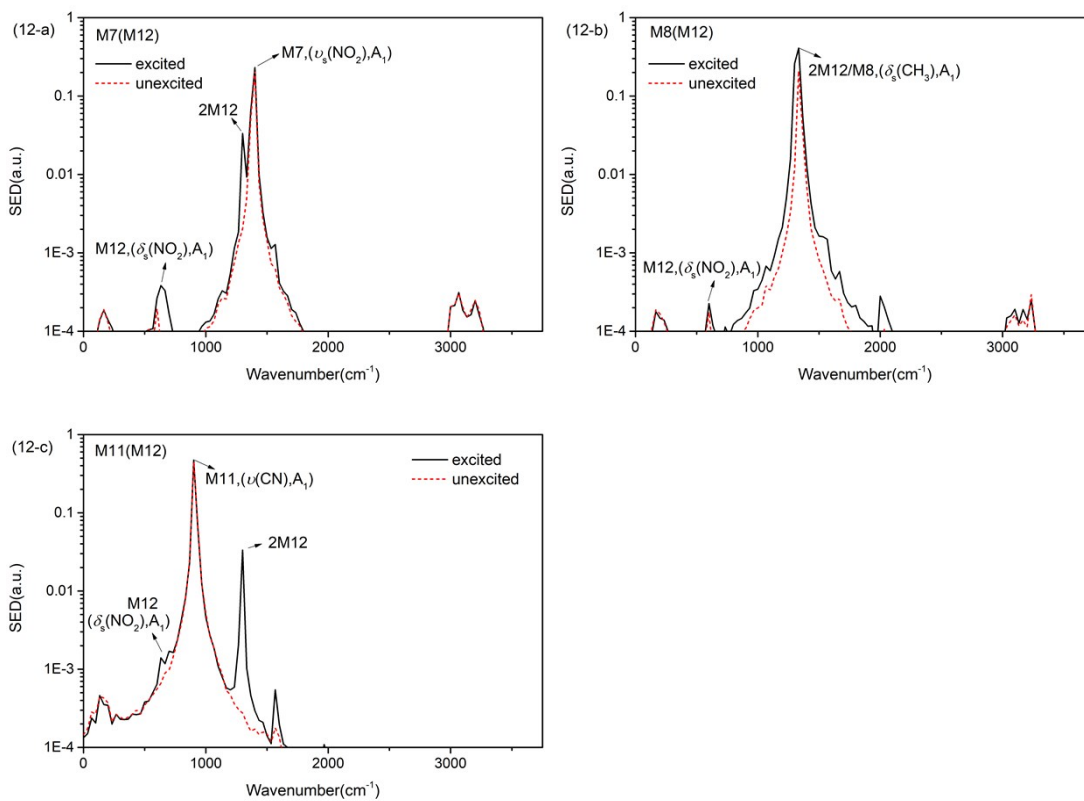
PM M10:



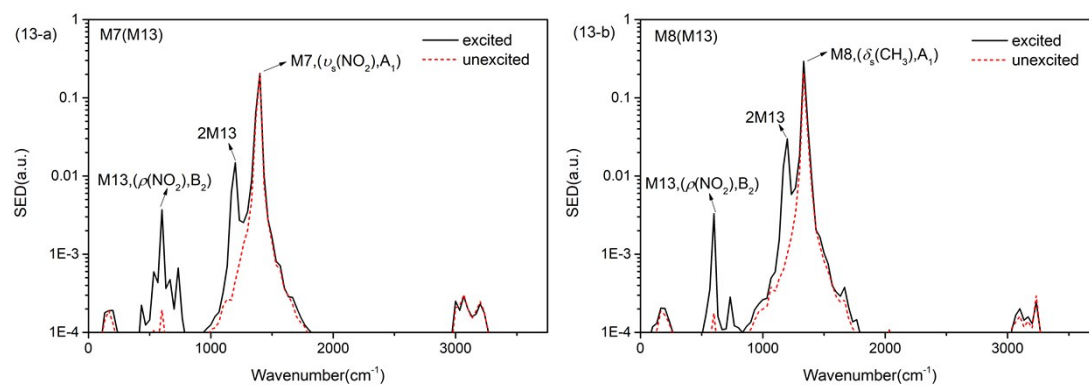
PM M11:



PM M12:



PM M13:



PM M14:

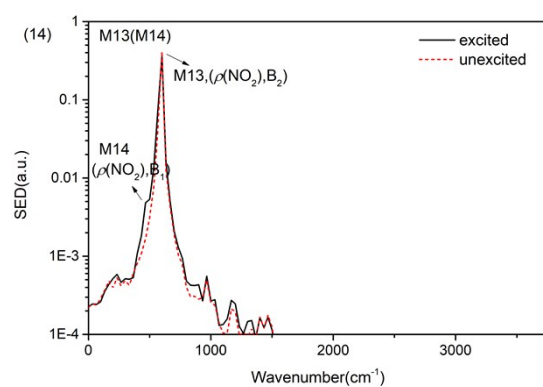


Figure S5. The spectra of the direct daughter modes in the first picosecond after the 14 selective excitations.